Vol. 11, No. 1, 2026, pp. 1-9
DOI: https://doi.org/10.29210/30036804000

Contents lists available at Journal ELORA

JRTI (Jurnal Riset Tindakan Indonesia)
ISSN: 2502-079X (Print) ISSN: 2503-1619 (Electronic)

Journal homepage: https://jrti.eloracenter.org/jrti

Superior microporous development in teak sawdust-derived activated carbon via N_2 activation for enhanced methylene blue uptake

I Gusti Agung Kade Suriadi[1], Dewa Ngakan Ketut Putra Negara[2], Tjokorda Gede Tirta Nindhia[3], I Gusti Agung Ketut Chatur Adhi Wirya Aryadi[4]

[1] Industrial Engineering Department, Faculty of Engineering, Udayana University
[2] Doctoral Study Program in Engineering Science, Faculty of Engineering, Udayana University
[3] Mechanical Engineering Department, Faculty of Engineering, Udayana University
[4] Mechanical Engineering, Faculty of Engineering, University of Mataram

Article Info

Article history:

Received Jan 21th, 2026
Revised Mar 18th, 2026
Accepted Mar 28th, 2026

Keyword:

Activated carbon,
Teak sawdust,
Nitrogen activation,
Carbon dioxide activation,
Microporous structure,
Methylene blue adsorption

ABSTRACT

This study investigates the effect of activation atmosphere (N_2 and CO_2) on the physicochemical properties and adsorption performance of teak sawdust-derived activated carbon for methylene blue removal. Carbonization was conducted at 750 °C followed by physical activation at 700 °C with a gas flow rate of 200 mL min^{-1}. Characterization results showed that N_2 activation produced a higher specific surface area and micropore volume compared to CO_2 activation, indicating more dominant microporous development. The N_2-activated sample exhibited superior adsorption uptake toward methylene blue under the tested condition (5 ppm), reaching 13.30 mg g^{-1}, while the CO_2-activated carbon showed lower uptake. The findings suggest that activation atmosphere strongly influences pore evolution and adsorption behavior. However, adsorption performance was evaluated at a single concentration; therefore, further isotherm and kinetic studies are required to determine the true maximum adsorption capacity and adsorption mechanism.

Corresponding Author:

I Gusti Agung Kade Suriadi,
Industrial Engineering Department, Faculty of Engineering, Udayana University
Email: gungsuriadi@yahoo.com

Introduction

Industrial wastewater from textile processes represents a major environmental challenge due to the presence of persistent synthetic dyes that resist natural degradation. Methylene blue is frequently used as a model contaminant because of its stability and toxicity, making it suitable for evaluating treatment technologies. Among various treatment methods, adsorption using activated carbon remains one of the most effective approaches due to its high efficiency, operational simplicity, and adaptability.

Biomass-derived activated carbon has gained increasing attention as a sustainable alternative to conventional commercial carbon. Lignocellulosic wastes such as agricultural residues are attractive precursors because they are abundant, low-cost, and rich in carbon content. Teak sawdust, a by-product of the wood industry, is particularly promising due to its high fixed carbon fraction and structural rigidity, which can support well-developed pore networks after thermal treatment.

The pore structure of activated carbon is strongly influenced by activation conditions, especially the activating atmosphere. Physical activation using CO_2 involves a mild gasification reaction ($C + CO_2 \rightarrow 2CO$) that gradually etches the carbon matrix, potentially widening existing pores. In contrast, N_2 acts as an inert atmosphere that primarily prevents oxidation and facilitates the removal of volatiles, which may favor micropore preservation. Despite these differences, comparative studies examining how these atmospheres influence pore evolution in teak sawdust-derived carbon remain limited. Therefore, this study aims to compare N_2 and CO_2 activation in terms of pore development, surface chemistry, and adsorption performance toward methylene blue. By clarifying the relationship between activation mechanism and adsorption behavior, this work contributes to the optimization of biomass-based activated carbon for wastewater treatment applications.

The textile industry is a vital sector of the economy, but its activities can have a negative impact on the environment. One such impact is water pollution due to the use of synthetic dyes such as methyl blue (Kuang et al., 2020). Methylene blue is frequently used in fabric dyeing due to its stability and bright color. However, 10-15% of the used dye is no longer usable and must be disposed of (Andri et al., 2019). The dye content in textile industry wastewater is around 20-30 mg/L, making it very difficult to decompose naturally Takanori et al., (1994) and causing serious environmental problems, including reduced water quality and adverse impacts on aquatic organisms (Dwiasi et al., 2018; Nabiilah et al., 2022; Tan et al., 2008).To reduce the methylene blue content in wastewater, one effective and economical method is adsorption, with activated carbon as an adsorbent (Ofgea et al., 2022; Putra Negara et al., 2023; Shipwiisho et al., 2023; Suriadi et al., 2024).

Activated carbon has a porous structure and high surface area, enabling it to efficiently adsorb organic compounds such as methyl blue. Activated carbon sources can be obtained from biomass (Arpan & Upendra, 2023; Bery et al., 2022; Choe et al., 2019; Putra Negara et al., 2023), such as bamboo , oil palm trunks Lin et al., (2020), palm kernel shells Rashidi & Yusup, (2017), brewed coffee waste (Mukherjee et al., 2022; Putra Negara et al., 2023, 2024), and teak dust waste, which are abundant and have not been optimally utilized (Nguyen et al., 2019; Putra Negara et al., 2024).

In the production of activated carbon from biomass, the precursor undergoes three stages: dehydration, carbonization, and activation. Dehydration aims to remove water and volatile compounds from the raw material, making it drier and more stable in subsequent processes. Carbonization involves the thermal decomposition of the raw material under an inert atmosphere, leading to the formation of char Karume et al., (2023) at temperatures of 300 to 800°C (Pallares et al., 2018) or 500 to 700°C (Li et al., 2008). The activation process is crucial for producing activated carbon with a well-developed pore structure, a high surface area, and optimal adsorption capacity (Allwar, 2012). This process can be achieved through physical or chemical activation methods. Physical activation involves treating carbonized materials with gases such as carbon dioxide (CO_2) or steam at high temperatures, typically 700-1,100°C (Bagheri & Shirpay, 2023). Chemical activation uses chemicals such as potassium hydroxide (KOH) or phosphoric acid (H_3PO_4) to activate the carbon at relatively lower temperatures, typically between 400 and 600°C (Allwar, 2012).

Activators, whether physical or chemical, determine the final characteristics of the resulting activated carbon. Activators affect pore size, pore distribution, and surface properties of the activated carbon, as well as its adsorption capacity. In this study, teak sawdust was converted into activated carbon using nitrogen and carbon dioxide as activating agents, and the resulting activated carbon was used for the adsorption of methyl blue. The specific objectives of this study were to determine the characteristics of activated carbon from teak sawdust activated with N_2 and CO_2, and how the adsorption capacities of teak sawdust activated with N_2 and CO_2 compare to methyl blue.

Method

Production of activated carbon

A total of 400 g of teak sawdust was dried in an electric furnace at 105 °C for 2 h to remove moisture. After drying, the sample was cooled to room temperature prior to carbonization. Carbonization was carried out in a tubular furnace under a continuous N_2 atmosphere to prevent oxidation. The furnace temperature was increased to 750 °C at a heating rate of 10 °C min^{-1} and maintained for 50 min. The carbonized product was then allowed to cool to room temperature inside the furnace and subsequently sieved to 60 mesh.

For activation, 40 g of the carbonized material was heated to 700 °C at a heating rate of 10 °C min^{-1} under a gas flow rate of 200 mL min^{-1}. Activation was conducted separately using N_2 and CO_2 gases with a purity of ≥ 99.9%. The temperature was maintained for 50 min before the sample was cooled to room temperature and stored in an airtight container. The selected carbonization (750 °C) and activation temperatures (700 °C) were chosen based on previous studies reporting effective pore development within this temperature range for lignocellulosic biomass precursors.

Characterization of activated carbon

The physicochemical properties of the samples were characterized using several analytical techniques. Surface morphology and pore structure were examined using Scanning Electron Microscopy (SEM). Proximate composition, including moisture, ash, volatile matter, and fixed carbon, was determined using Thermogravimetric Analysis (TGA) in accordance with ASTM D7582. Surface functional groups were identified using Fourier Transform Infrared (FTIR) spectroscopy. Textural properties, including specific surface area, pore volume, pore diameter, and pore size distribution, were determined from nitrogen adsorption–desorption isotherms using BET analysis. Crystallinity and structural ordering were evaluated using X-Ray Diffraction (XRD).

Methylene blue adsorption test

Adsorption experiments were conducted using a 5 ppm methylene blue solution. A total of 0.1 g of activated carbon was added to 20 mL of solution and stirred for 20 min, followed by equilibration for 2 h. The mixture was filtered, and the residual dye concentration was measured at 664 nm using a UV–Vis spectrophotometer. The adsorption value obtained in this study represents adsorption uptake at the tested condition. Since the experiment was performed at a single initial concentration, the reported value does not represent the maximum adsorption capacity (Qmax). Determination of Qmax would require adsorption isotherm experiments at multiple concentrations. The amount of adsorption was calculated using equation (1) (Choi & Yu, 2019):

$$q_{t=\frac{(C_0-C_t}{m})V} \quad (1)$$

where Co (mg/L) is the initial concentration of the solution, Ct (mg/L) is the concentration of the solution at time t, V (L) is the volume of the solution, and m (g) is the mass of activated carbon. The percentage of methyl blue absorption was calculated using equation (2) (Choi & Yu, 2019):

$$\%_{ads} = \frac{C_0 - C_f}{C_0} x\ 100\%$$

Results and Discussions

Proximate analysis

In the proximate composition data, all samples showed almost the same moisture content (≈8– 10%). The carbonization result (CHAR) had the highest volatile matter (11.58%) and the lowest fixed carbon (69.7%). After the activation process at 700 °C with both CO_2 and N_2, there was a reduction in volatile matter and an increase in fixed carbon: TS-CO_2 showed 9.00% volatile and the highest fixed carbon of 75.74%, while TS-N_2 had 10.46% volatile and 74.08% fixed carbon. Ash decreased most significantly in TS-N_2 (5.41%) compared to CHAR (9.92%), while TS-CO_2 had medium ash (6.96%). Overall, activation increases the remaining carbon fraction (activated carbon quality) and reduces the ash fraction and unwanted volatile substances. The TGA composition of the activated carbon produced meets the Indonesian National Standard (SNI 06-3730-1995) for powdered activated carbon. This standard states that powdered activated carbon must not have a volatile substance content above 25%, a moisture content above 15%, or an ash content above 10%, while maintaining a minimum carbon content of 65%.

Table 1. Proximate composition as a TGA result

Sampel	Proximate Composition			
	Moisture (%)	Volatile (%)	Ash (%)	Fix Carbon (%)
CHAR	8,8	11,58	9,92	69,7
TS-CO2	8,3	9	6,96	75,74
TS-N2	10,05	10,46	5,41	74,08

FTIR analysis

From the FTIR spectra, all samples showed characteristic bands of biomass/carbon. The broad band around 3200–3600 cm^{-1} indicates O–H groups (bound water or alcohol/phenol), the band near 2900 cm^{-1} indicates C–H stretching (alkyl residue), the band at ~1700 cm^{-1} indicates C=O groups (carbonyl/ester/ketone), and the band in the range of 1600–1500 cm^{-1} is generally related to aromatic skeletal stretching (C=C). In the region of 1200–1000 cm^{-1}, there are contributions of C–O (ester, ether) and other oxygen groups. Changes after activation showed that the intensity of the O–H and C=O bands tended to decrease in the activated samples (especially in TS-N_2), indicating deoxygenation and increased carbonicity/aromaticity; TS-CO_2 appears to retain some oxygen groups (the C–O band is relatively clearer), suggesting its surface likely has more bound oxygen functionalities useful for adsorption of polar substances. The sharp peak at ~1400–1500 cm^{-1} likely originates

from aromatic vibrations or instrument artifacts. The relative shifts and intensity changes between samples indicate surface chemical modifications due to activation.

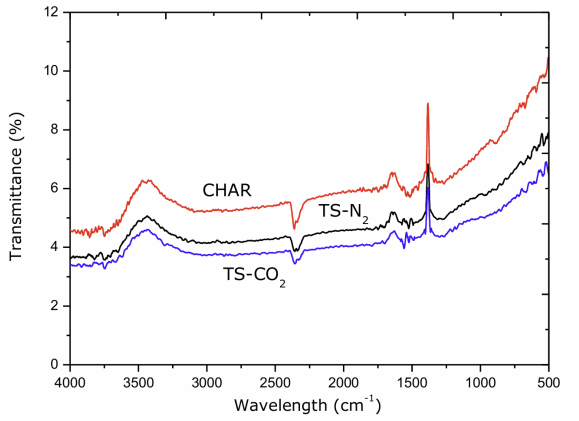

Figure 1. FTIR spectra of sample

Activation at 700°C improved the quality of activated carbon from teak sawdust compared to raw char, as indicated by higher fixed carbon and lower volatile/ash content. TS-CO_2 produced slightly higher fixed carbon and retained some surface oxygen groups (useful for polar adsorption), while TS-N_2 produced the lowest ash and the highest degree of deoxygenation (a more aromatic/less polar surface). Therefore, the choice between CO_2 and N_2 activation should be based on the final application. CO_2 is for the adsorption of polar/ionic compounds (more functional groups), while N_2 is for applications requiring carbon with low ash purity and chemical stability.

Adsorption isotherm

The graph in Figure 2 shows nitrogen adsorption isotherms (BET analysis), indicating the ability of the samples (Char, TS-CO_2, TS-N_2) to adsorb nitrogen gas at various relative pressures (P/Po). The graph clearly shows that the activated samples (TS-N_2 and TS-CO_2) have a much higher nitrogen adsorption capacity than the raw char. This indicates the formation of new pores after the activation process, which increases the specific surface area. TS-N_2 exhibits the highest curve (up to >35 cc/g), followed by TS-CO_2 (~25 cc/g), while char only reaches around 12 cc/g.The continuously increasing curve pattern without a plateau until the P/Po approaches 1 indicates that this material is predominantly mesoporous (2–50 nm). Activation with N_2 at 700°C produces a more developed porous structure than activation with CO_2. This is consistent with previous proximate data, where TS-N_2 had a lower ash content, resulting in more open pores. Meanwhile, activation with CO_2 still resulted in a significant increase in surface area, but not as high as for TS-N_2, likely due to the pores being partially covered by the remaining oxygen groups. Overall, these isotherm results confirm that the activation process can increase the specific surface area and adsorption capacity. TS-N_2 was the sample with the highest adsorption capacity. TS-N_2 exhibited the highest adsorption performance, which can be attributed to its higher surface area and micropore dominance. However, further studies using different adsorbates and phases are required to evaluate its suitability for specific adsorption applications.

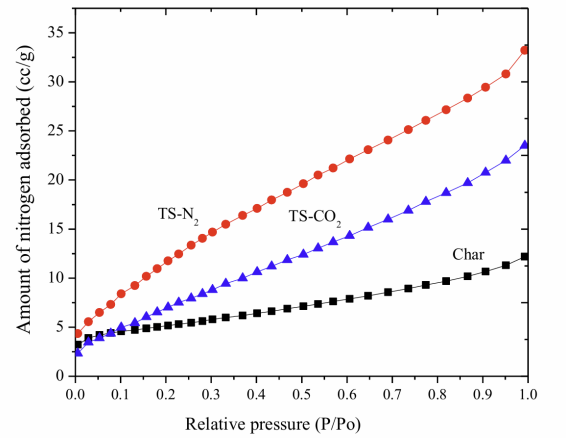

Figure 2. Adsorption isotherm

Pore size distribution

The graph in Figure 3 shows the pore size distribution (PSD) based on nitrogen adsorption. This graph shows how activated carbon has different pore characteristics than raw char. The char (black) shows a shallow and shallow pore distribution, dominated by macropores with a very limited number of micropores. This explains the low nitrogen adsorption capacity in the previous isotherm analysis.

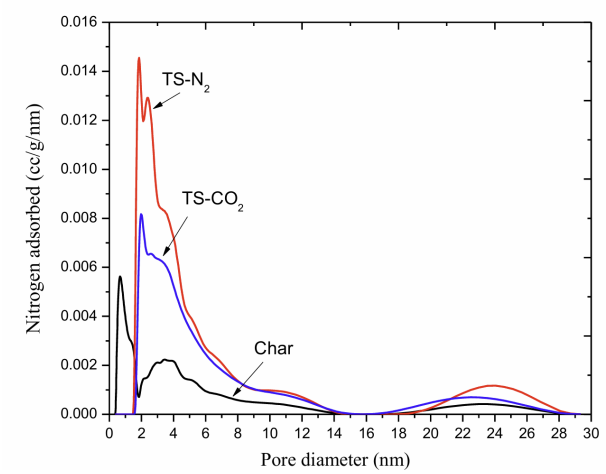

Figure 3. Pore size distribution

The difference in pore characteristics between N_2- and CO_2-activated carbons can be explained by their distinct activation mechanisms. CO_2 activation involves a gasification reaction with carbon atoms, which progressively removes carbon from pore walls. This process can generate new micropores but also enlarge existing ones into mesopores, resulting in a broader pore size distribution.

In contrast, N_2 is an inert gas that does not react with carbon at the activation temperature. Its primary role is to create an oxygen-free environment and facilitate the removal of volatile compounds generated during thermal decomposition. This condition helps preserve the carbon framework and promotes the formation of a more dominant microporous structure, which explains the higher surface area and micropore volume observed in the N_2-activated sample.

The superior adsorption uptake of the N_2-activated carbon can therefore be attributed to the greater availability of micropores, which are particularly effective for adsorbing small dye molecules such as methylene blue through pore-filling mechanisms. This mechanistic interpretation is consistent with the pore size distribution results shown in Figure 3.

After activation with both CO_2 (blue) and N_2 (red), new pores form, dominated by the micropore range (2–4 nm). The distribution peak for TS-N_2 is sharper and higher than that for TS-CO_2, indicating that activation with N_2 results in a greater number of micropores. These micropores play a significant role in increasing the specific surface area and gas adsorption capacity. Furthermore, both TS-N_2 and TS-CO_2 also show contributions from mesopores (10–30 nm), although their intensities are lower than those of micropores.

The presence of mesopores is essential for the diffusion of larger molecules, thus facilitating access into the microporous structure. Combining these isotherm results and pore size distributions, it is clear that activation with N_2 at 700°C produces activated carbon with the best microporous structure for gas or vapor adsorption applications, while activation with CO_2 produces a mixed pore structure (micro + meso) that is more suitable for the adsorption of polar or medium-sized molecules.

Surface morphology

Figure 4(a) shows the char surface, which still appears relatively dense and less porous. Cracks and layers indicate carbonization, but no significant voids have formed. The EDX spectrum shows the dominant presence of C, but also strong peaks from impurities such as O, Si, Ca, K, and Mg. This indicates that the char still contains significant amounts of minerals (ash) that have not yet been removed.

The TS-CO_2 in Figure 4b shows that after CO_2 activation, the surface becomes more open and pores begin to form, although they are not yet uniform. The texture appears rougher than the char texture, indicating etching due to partial CO_2 gasification. The carbon content remains high, but the O signal is more pronounced than that of TS-N_2. This is consistent with previous FTIR analysis, which found that CO_2 activation tends to retain oxygen

functional groups on the surface. Ash elements (Ca, K, Si) are still present but are slightly less intense than those of the char. Surface morphology of the sample is shown in Figure 4.

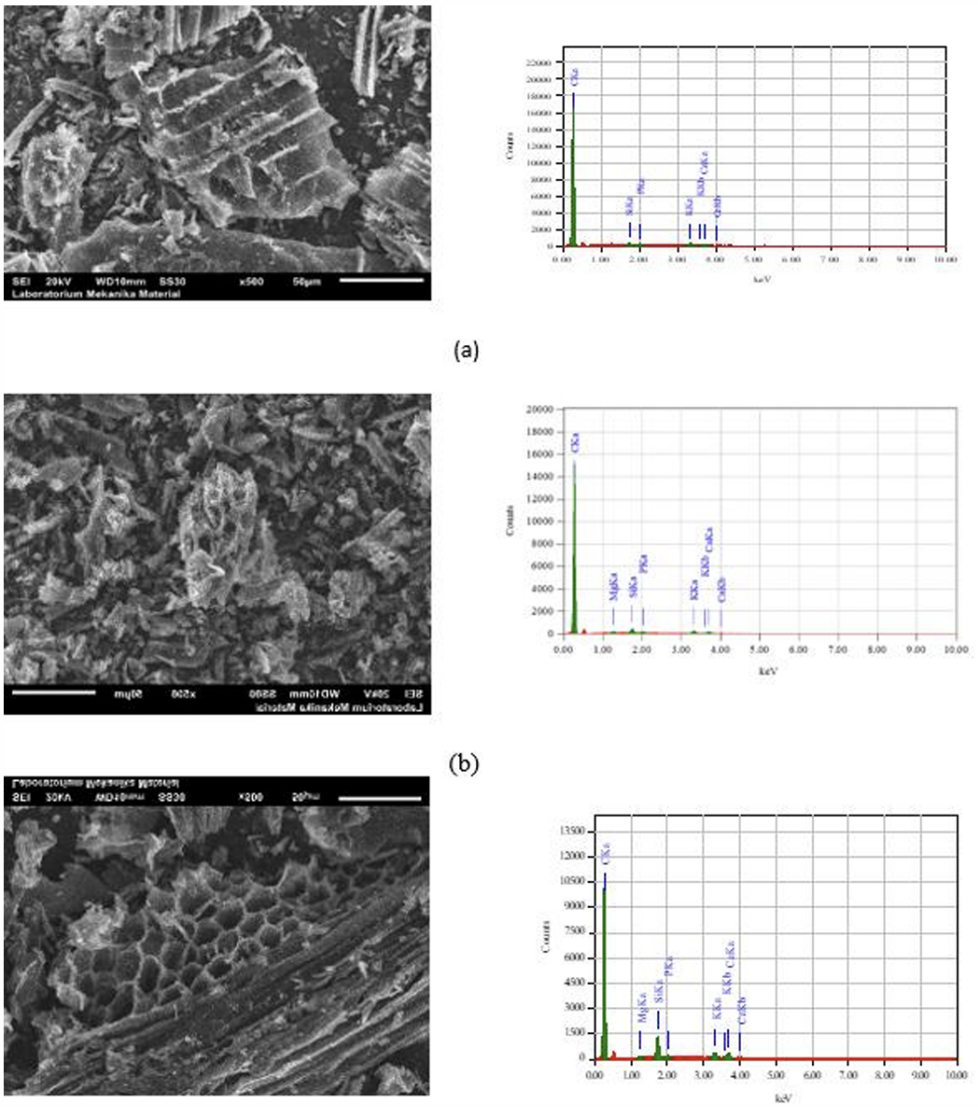

Figure 4. Surface morphology (a) Char, (b) TS-CO2, (c) TS-N2

The TS-N_2 sample in Figure 4c shows that the N_2-activated surface has a more porous structure, with a better distribution of small cavities (micropores). This is in line with the results of BET and PSD analysis, which showed the highest nitrogen adsorption capacity. The EDX spectrum shows a dominance of carbon with a lower oxygen peak than TS-CO_2, indicating a more deoxygenated surface. Ash/mineral elements (Ca, K, Si) are less than char and TS-CO_2, indicating more effective surface cleaning.

Pore structure

The carbonized carbon (char) has a very low specific surface area (SSR) of 8.4 m²/g. This value indicates that pore development has hardly occurred in the sample. The pore volume (Vp) is also small, at only 0.010 cc/g, consistent with SEM results and nitrogen adsorption isotherms. The average pore diameter (Dp) of 2.90 nm is indeed within the mesoporous range, but due to the very limited number of pores formed, their contribution to adsorption capacity is also low. After activation with CO_2 gas, the pore characteristics improved significantly. The specific surface area increased almost fourfold to 30.79 m²/g, indicating that partial gasification with CO_2 opened the pore structure and expanded the carbon surface area.

The pore volume also increased to 0.0364 cc/g, although not as large as in N_2 activation. Meanwhile, the average pore diameter decreased to 2.36 nm, indicating that the majority of the pores formed were micropores with a small addition of mesopores. The activated carbon activated with N_2 gas exhibited the best pore characteristics among the three samples. The specific surface area reached 51.2 m²/g, about six times that of

char, indicating excellent pore structure development. The pore volume was also the highest, at 0.0514 cc/g, indicating this sample could accommodate a larger number of adsorbate molecules. The average pore diameter of 2.08 nm, the smallest among all samples, indicated the dominance of micropores in the activated carbon's pore structure.

Table 2. Pore structure

		Surface Structure	
Sample	**S_{BET} (m2/g)**	**Vp (cc/g)**	**Dp (nm)**
CHAR	8.400	0.010	2.900
TS-CO_2	30.79	0.0364	2.36
TS-N_2	51.2	0.0514	2.08

Methylene blue adsorption performance

Adsorption of methylene blue by activated carbon is shown in Table 3 and Figure 5. Char-derived carbon (char) has a very low methylene blue adsorption capacity of only 4.11 mg/g. This value is consistent with its small specific surface area (8.4 m²/g) and underdeveloped pores, making it ineffective as a dye adsorbent. After activation with CO_2, the adsorption capacity increased significantly to 11.59 mg/g, nearly three times that of char. This increase is consistent with the increased surface area (30.79 m²/g) and larger pore volume. Furthermore, the presence of oxygen groups on the surface of the CO_2-activated carbon contributes significantly through electrostatic interactions with the cationic methylene blue molecules.

Therefore, TS-CO_2-activated carbon has a balance between surface area and the presence of active functional groups, making it more suitable for the adsorption of polar dyes. N_2-activated carbon performed best, with a methylene blue adsorption capacity of 13.30 mg/g, the highest among all samples. This is consistent with the highest specific surface area (51.2 m²/g), the largest pore volume (0.0514 cc/g), and the dominance of micropores, which play a significant role in adsorption. Although TS-N_2 has fewer surface oxygen groups than TS-CO_2, its large micropores predominate, resulting in superior adsorption capacity. Therefore, TS-N_2 is more suitable for adsorption applications requiring maximum capacity.

Overall, the results of the methylene blue adsorption test demonstrate that activation successfully improves the quality of activated carbon from teak sawdust waste. Char serves only as a starting material with low capacity, while TS-CO_2 provides significant improvements, particularly for the adsorption of polar compounds. While TS-N_2 excels due to its large surface area and pore count. These data are consistent with previous analyses (TGA, FTIR, BET, PSD, SEM-EDX), which demonstrated that activation significantly improves the pore structure and adsorption capacity of activated carbon.

Table 3. Adsorption capacity of the sample on the methylene blue

	Methylene Blue Adsorbed (mg/g)				
Sample	**Run 1**	**Run 2**	**Run 3**	**Average**	**Standard Deviation**
CHAR	4.06	4.15	4.12	4.11	0.05
TS-CO_2	11.38	11.80	11.59	11.59	0.21
TS-N_2	13.50	13.02	13.38	13.30	0.25

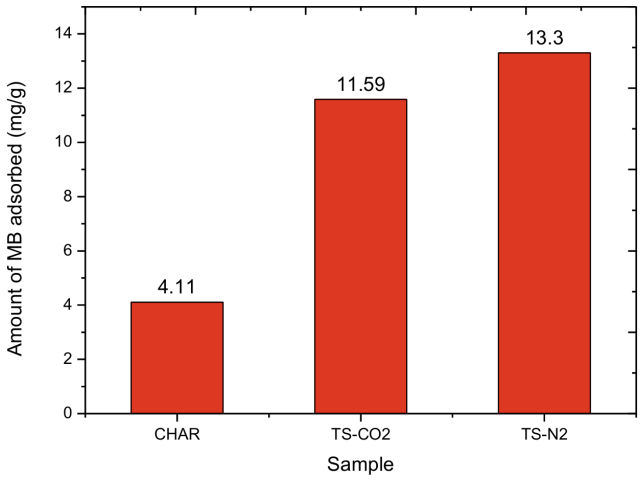

Figure 5. Adsorption capacity

Conclusions

This study demonstrates that activation atmosphere plays a crucial role in determining the physicochemical properties of teak sawdust-derived activated carbon. N_2 activation produced a higher specific surface area and micropore volume compared to CO_2 activation, resulting in greater methylene blue adsorption uptake under the tested condition. These findings highlight the importance of controlling activation conditions to tailor pore structure for targeted adsorption applications and support the potential of teak sawdust as a valuable biomass precursor for wastewater treatment materials. However, the adsorption performance was evaluated at a single initial concentration, and therefore the reported value represents adsorption uptake rather than maximum capacity. Future research should include full adsorption isotherm, kinetic, and thermodynamic analyses to better understand the adsorption mechanism and practical applicability of the material.

Acknowledgments

Deep gratitude is expressed to Udayana University through the Institute for Research and Community Service (LPPM), which has funded this research through contract number: B/229.517/UN14.4.A/PT.01.03/2025.

References

Allwar, A. (2012). Characteristics Of Pore Structures And Surface Chemistry Of Activated Carbons By Physisorption, Ftir And Boehm Methods. Iosr Journal Of Applied Chemistry, 2(1), 9–15.

Andri, R., Ervan, S., Setiaty, P., & Halimatuddahliana. (2019). Pengaruh Waktu Kontak Dan Massa Adsorben Biji Asam Jawa (Tamarindus Indica) Dengan Aktivator H3po4 Terhadap Kapasitas Adsorpsi Zat Warna Methylene Blue. Jurnal Teknik Kimia Usu, 8(2), 54–60. Https://Doi.Org/10.32734/Jtk.V8i2.1881

Arpan, H., & Upendra, K. (2023). Application Of Taguchi Methodology In Adsorption Of Malachite Green Dye Using Chemically Enhanced Bambusa Tulda (Indian Timber Bamboo). Advances In Environmental Technology, 9(2), 99–111. Https://Doi.Org/10.22104/Aet.2023.5907.1622

Bagheri, S. K. S. M. M., & Shirpay, M. A. (2023). Effect Of Physical And Chemical Activation Methods On The Structure, Optical Absorbance, Band Gap And Urbach Energy Of Porous Activated Carbon. Sn Applied Sciences, 5, 313. Https://Doi.Org/10.1007/S42452-023-05559-6

Bery, H. M. E., Saleh, M., Gendy, R. A. E., Saleh, M. R., & Thabet, S. M. (2022). High Adsorption Capacity Of Phenol And Methylene Blue Using Activated Carbon Derived From Lignocellulosic Agriculture Wastes. Scientific Report, 1–17. Https://Doi.Org/10.1038/S41598-022-09475-4

Choe, U., Mustafa, A. M., Lin, H., Xu, J., & Sheng, K. (2019). Effect Of Bamboo Hydrochar On Anaerobic Digestion Of Fish Processing Waste For Biogas Production. Bioresource Technology, 283, 340–349. Https://Doi.Org/10.1016/J.Biortech.2019.03.084

Choi, H. J., & Yu, S. W. (2019). Biosorption Of Methylene Blue From Aqueous Solution By Agricultural Bioadsorbent Corncob. Environmental Engineering Research, 24, 99–106. Https://Doi.Org/10.4491/Eer.2018.107

Dwiasi, D. W., Setyaningtyas, T., & Riyani, K. (2018). Penurunan Kadar Metilen Biru Dalam Limbah Batik Sokaraja Menggunakan System Fe2o3-H2o2-Uv. Jurnal Rekayasa Kimia Dan Lingkungan, 13(1), 78–86. Https://Doi.Org/10.23955/Rkl.V12i1.10572

Karume, I., Bbumba, S., Tewolde, S., Mukasa, I. Z. T., & Ntale, M. (2023). Impact Of Carbonization Conditions And Adsorbate Nature On The Performance Of Activated Carbon In Water Treatment. Bmc Chemistry, 17, 162–172. Https://Doi.Org/10.1186/S13065-023-01091-1

Kuang, Y., Zhang, X., & Zhou, S. (2020). Adsorption Of Methylene Blue In Water Onto Activated Carbon By Surfactant Modification. Water, 12, 1–19. Https://Doi.Org/10.3390/W12020587

Li, W., Yang, K., Peng, J., Zhang, L., Guo, S., & Xia, H. (2008). Effects Of Carbonization Temperatures On Characteristics Of Porosity In Coconut Shell Chars And Activated Carbons Derived From Carbonized Coconut Shell Chars. Industrial Crops And Products, 8, 190–198. Https://Doi.Org/10.1016/J.Indcrop.2008.02.012

Lin, J., Choowang, R., & Zhao, G. (2020). Fabrication And Characterization Of Activated Carbon Fibers From Oil Palm Trunk. Polymer, 12, 2775–2784. Https://Doi.Org/10.3390/Polym12122775

Nabiilah, C. P. R., Yudoyono, G., & Indarto, B. (2022). Peningkatan Degradasi Larutan Metilen Biru Menggunakan Lapisan Tio2 Pada Reaktor Calma Melalui Bentuk Penataan Substrat. Sains Dan Seni Its, 11(5), 2337–2520.

Nguyen, H. D., Tran, H. N., Chao, H., & Lin, C. (2019). Activated Carbons Derived From Teak Sawdust-Hydrochars For Efficient Removal Of Methylene Blue, Copper, And Cadmium From Aqueous Solution. Water, 11, 1–15. Https://Doi.Org/10.3390/W11122581

Ofgea, N. M., Tura, A. M., & Fanta, G. M. (2022). Activated Carbon From H3po4-Activated Moringa Stenopetale Seed Husk For Removal Of Methylene Blue: Optimization Using The Response Surface Method (Rsm). Environmental And Sustainability Indicators, 16, 1–14. Https://Doi.Org/10.1016/J.Indic.2022.100214

Pallares, J., Gonzalez-Cencerrado, A., & Arauzo, I. (2018). Production And Characterization Of Activated Carbon From Barley Straw By Physical Activation With Carbon Dioxide And Steam. Biomass And Bioenergy, 115, 64–73. Https://Doi.Org/10.1016/J.Biombioe.2018.04.015

Putra Negara, D. N. K., Nindhia, T. G. T., Widiyarta, I. M., Karohika, I. M. G., Suarda, M., & Dwijana, I. G. K. (2023). Characteristics And Performance Analysis Of Activated Carbons Derived From Different Precursors And Activators For Waste Water Adsorption. Eureka: Physics And Engineering, 6, 160–172. Https://Doi.Org/10.21303/2461-4262.2023.003116

Putra Negara, D. N. K., Widiyarta, I. M., Gatot, I. M., Agung, I. G., Suriadi, K., Dwijana, I. G. K., Lokantara, I. P., Parwata, I. M., & Suarsana, I. K. (2024). Preparation And Characterization Of Pelleted And Powdered Activated Carbons Derived From Used Brewed Coffee. Trends In Sciences, 20(12), 1–11. Https://Doi.Org/10.48048/Tis.2024.7136

Rashidi, N. A., & Yusup, S. (2017). Potential Of Palm Kernel Shell As Activated Carbon Precursors Through Single Stage Activation Technique For Carbon Dioxide Adsorption. Journal Of Cleaner Production, 168, 474–486. Https://Doi.Org/10.1016/J.Jclepro.2017.09.045

Shipwiisho, L., Rahman, A., Ndakola, M., Kapolo, P., Uahengo, V., & Babu, S. (2023). The Production Of Activated Carbon From Acacia Erioloba Seedpods Via Phosphoric Acid Activation Method For The Removal Of Methylene Blue From Water. Bioresource Technology Reports, 23, 101568. Https://Doi.Org/10.1016/J.Biteb.2023.101568

Suriadi, I. G. A. K., Putra Negara, D. N. K., Nindhia, T. G. T., Atmika, I. K. A., Dwi, I. M., Penindra, I. M. D. B., & Karohika, I. M. G. (2024). The Impact Of Activation Heating Rate On Pore Structure In Teak Sawdust-Derived Activated Carbon And Its Application In Methylene Blue Adsorption. Trends In Sciences, 21(9), 8110. Https://Doi.Org/10.48048/Tis.2024.8110

Takanori, T., Mie, W., Katsumi, O., Akira, Y., Shunro, K., & Toshishiko, O. (1994). Antioxidative Components Isolated From The Seed Of Tamarind (Tamarindus Indica L). Journal Of Agricultural And Food Chemistry, 42, 2671–2674. Https://Doi.Org/10.1021/Jf00048a004

Tan, I. A. W., Ahmad, A. L., & Hameed, B. H. (2008). Adsorption Of Basic Dye On High-Surface-Area Activated Carbon Prepared From Coconut Husk: Equilibrium, Kinetic And Thermodynamic Studies. Journal Of Hazardous Materials, 154, 337–346. Https://Doi.Org/10.1016/J.Jhazmat.2007.10.031